

Characterization of a Streptococcal Cholesterol-Dependent Cytolysin with a Lewis y and b Specific Lectin Domain[†]

Stephen Farrand,[‡] Eileen Hotze,[‡] Paul Friese,[§] Susan K. Hollingshead,^{||} David F. Smith,[⊥] Richard D. Cummings,[⊥] George L. Dale,[§] and Rodney K. Tweten^{*‡}

Department of Microbiology and Immunology and Department of Medicine, University of Oklahoma Health Sciences Center, Oklahoma City, Oklahoma 73104, Department of Microbiology, University of Alabama at Birmingham, Birmingham, Alabama 35294-2170, and Department of Biochemistry, Emory University School of Medicine, Atlanta, Georgia 30322

Received April 3, 2008; Revised Manuscript Received May 6, 2008

ABSTRACT: The cholesterol-dependent cytolysins (CDCs) are a large family of pore-forming toxins that often exhibit distinct structural changes that modify their pore-forming activity. A soluble platelet aggregation factor from *Streptococcus mitis* (Sm-hPAF) was characterized and shown to be a functional CDC with an amino-terminal fucose-binding lectin domain. Sm-hPAF, or lectinolysin (LLY) as renamed herein, is most closely related to CDCs from *Streptococcus intermedius* (ILY) and *Streptococcus pneumoniae* (pneumolysin or PLY). The LLY gene was identified in strains of *S. mitis*, *S. pneumoniae*, and *Streptococcus pseudopneumoniae*. LLY induces pore-dependent changes in the light scattering properties of the platelets that mimic those induced by platelet aggregation but does not induce platelet aggregation. LLY monomers form the typical large homooligomeric membrane pore complex observed for the CDCs. The pore-forming activity of LLY on platelets is modulated by the amino-terminal lectin domain, a structure that is not present in other CDCs. Glycan microarray analysis showed the lectin domain is specific for difucosylated glycans within Lewis b (Le^b) and Lewis y (Le^y) antigens. The glycan-binding site is occluded in the soluble monomer of LLY but is apparently exposed after cell binding, since it significantly increases LLY pore-forming activity in a glycan-dependent manner. Hence, LLY represents a new class of CDC whose pore-forming mechanism is modulated by a glycan-binding domain.

The viridans streptococci, which include *Streptococcus mitis*, *Streptococcus mutans*, *Streptococcus salivarius*, and *Streptococcus sanguis*, are normally found as members of the normal flora of the oropharynx. These organisms can escape this niche, however, and cause a variety of diseases that include infective endocarditis, bacteremia, and septicemia. *S. mitis* is one of the more common isolates, and its antibiotic resistance is increasing, making treatment of its infections difficult (1–4). *S. mitis* was recently associated with a large outbreak of a toxic shock-like syndrome that affected thousands of individuals in China (5). *S. mitis* is typically not considered to be toxigenic, and it is characterized by an α -hemolytic phenotype. Jeffries et al. (6), however, recently showed that some *S. mitis* strains express a cholesterol-dependent cytolysin (CDC), designated mitilysin (MLY), which is nearly identical to *Streptococcus pneumoniae* pneumolysin. Another potential *S. mitis* pathogenesis factor is human platelet aggregation factor (Sm-

hPAF)¹ that was purified from *S. mitis* isolated from a patient with Kawasaki disease (7). This protein was shown to aggregate human platelets and was designated *S. mitis* human platelet aggregation factor or Sm-hPAF. More recently, Ohkuni et al. (8) showed that antibody titers to a Sm-hPAF-derived peptide were significantly elevated in children with Kawasaki disease, a disease that is often associated with platelet aggregation and coronary artery thrombosis.

The peptide sequence reported by Ohkuni et al. (8) was derived from the sequence for a Sm-hPAF gene from *S. mitis* Nm-65 recently reported in GenBank (accession number AB051299.1). The sequence of Sm-hPAF encodes a predicted CDC structure that is most closely related to intermedilysin (ILY), the CDC from *Streptococcus intermedius* (9). The DNA-derived primary structure of Sm-hPAF exhibits an extra amino-terminal domain of about 162 amino acids. Based on the DNA-derived primary structure, this domain is related to the European eel *Anguilla anguilla* agglutinin (AAA), a fucose-binding lectin that preferentially binds glycans containing fucosylated structures found in the blood group antigens A, B, H, and Lewis a (Le^a) (10, 11).

Herein we describe the properties of purified recombinant Sm-hPAF (referred to as lectinolysin or LLY hereafter) from *S. mitis* SK597. These studies show that LLY is a pore-forming CDC with a functional glycan-binding domain. LLY

[†] This work was supported by a grant from the National Institute of Allergies and Infectious Diseases (AI037657) and in part by NIGMS—The Consortium for Functional Glycomics (GM62116).

* Corresponding author. Phone: (405) 271-1205ext 1. Fax: (405) 271-3117. E-mail: rod-tweten@ouhsc.edu.

[‡] Department of Microbiology and Immunology, University of Oklahoma Health Sciences Center.

[§] Department of Medicine, University of Oklahoma Health Sciences Center.

^{||} Department of Microbiology, University of Alabama at Birmingham.

[⊥] Department of Biochemistry, Emory University School of Medicine.

¹ Abbreviations: ILY, intermedilysin; PLY, pneumolysin; PFO, perfringolysin; Sm-hPAF, *Streptococcus mitis* human platelet aggregation factor; EC₅₀, half-maximal effective concentration.

does not trigger platelet aggregation but does form pores in platelet membranes. The isolated fucose-binding lectin domain of LLY exhibits specificity for glycans containing the Lewis y (Le^y) and b (Le^b) antigens. The lectin domain of LLY appears to modulate the pore-forming activity of LLY in a glycan-dependent manner after LLY binds to the cell surface.

METHODS

Bacterial Strains, Plasmids, and Chemicals. The full-length gene for LLY was cloned by PCR from the chromosomal DNA of *S. mitis* strain SK597 using the primer ATGAATCAAGAAAAACGTTTGCATCGCTTTGTCAAAAAG, and the reverse primer sequence was 5'-TTACTCATTCACAATTTTTCATCAACTTTAGGGTTTAG. For purposes of expression the cloned LLY gene was amplified with the primers 5'-TCG-GATCCGAGCAAGGGAATCGTCCAGTTG that introduced a 5' *Bam*HI endonuclease site and 5'-CTGAATTCCTTACTCATTCACAATTTTTCATCAACTTTAGGG that placed a 3' *Eco*RI endonuclease after the stop codon at the 3' end of the gene. These primers removed the signal peptide and placed the gene for the secreted LLY in-frame in the pTrcHisA vector (Invitrogen). ILY and PFO were previously cloned into pTrcHisA as described (12, 13). All mutations were made in the native LLY (naturally cysteine-less), ILY (naturally cysteine-less), or cysteine-less PFO (PFO^{C459A}) background. All chemicals and enzymes were obtained from Sigma, VWR, or Research Organics. All fluorescent probes were obtained from Molecular Probes (Invitrogen).

Generation and Purification of Recombinant LLY, ILY, and PFO and Their Derivatives. Using PCR QuikChange mutagenesis (Stratagene), various amino acid substitutions were introduced into native LLY, ILY, or PFO^{C459A}. The Oklahoma Medical Research Foundation Core DNA Sequencing Facility performed all DNA sequence analysis. The expression and purification of recombinant LLY, ILY, PFO, and their derivatives from *Escherichia coli* were performed as described (13, 14). Purified protein was dialyzed into buffer [300 mM NaCl, 10 mM MES, 1 mM EDTA (pH 6.5)] overnight at 4 °C, made 5 mM in dithiothreitol (DTT) and 10% (v/v) sterile glycerol, and stored at -80 °C. For mutants that contained an engineered disulfide bridge the DTT was left out of the storage buffer.

PCR Screening Streptococci for the LLY Gene. Primers were used in the PCR amplification at a 20 pmol final concentration. These primers were designed to amplify out the entire coding sequence for the LLY gene. The forward primer sequence was 5'-ATGAATCAAGAAAAACGTTTGCATCGCTTTGTCAAAAAG, and the reverse primer sequence was 5'-TTACTCATTCACAATTTTTCATCAACTTTAGGGTTTAG. Chromosomal DNA from each streptococcal strain was prepared using the Invitrogen Easy DNA kit, and 100 ng was added to the PCR reaction. An additional 2 μ L of 25 mM MgCl₂ was added to Qiagen Master Mix for a final PCR volume of 25 μ L. Each PCR product was separated on a 1% agarose gel.

Chemical Modification of LLY and Its Derivatives with Sulfhydryl-Specific Fluorescent Probes. The cysteine derivatives of LLY and LLY^{Lec} were modified with Alexa Fluor 488 C₅-maleimide (Invitrogen) via the sulfhydryl group as previously described (12). Modified protein stocks were

adjusted to 10% (v/v) sterile glycerol, quick frozen in liquid nitrogen, and stored at -80 °C. Proteins were labeled at an efficiency of 75% or greater.

K_d Determination. Fluorescein-labeled glycans were prepared as previously described using free reducing oligosaccharides (15). The K_d of the interaction of LLY^{Lec} with Le^y was determined by fluorescence anisotropy. Fluorescence measurements were carried out using an SLM 8100 fluorometer equipped with excitation and emission calcite polarizers. The excitation and emission monochromator wavelengths were set to 480 and 520 nm, respectively. The excitation and emission bandpass was set to 4 nm. Sample volume was maintained at 300 μ L in a Starra microcell with a total capacity of 560 μ L. Temperature was maintained at 23 °C. The fluorescein-labeled Le^y was maintained at 167 nM, and the LLY^{Lec} was varied from 300 nM to 120 μ M. The anisotropy (*r*) was calculated at each concentration of LLY from the equation:

$$r = \frac{I_{VV} - GI_{VH}}{I_{VV} + 2GI_{VH}}$$

I is intensity, *V* is vertically polarized light, and *H* is horizontally polarized light. The *G* factor ($G = I_{HV}/I_{HH}$) was calculated for each sample. The Δr was plotted versus the concentration of LLY, and the dissociation constant (*K_d*) was calculated using the equation $Y = B_{\max}X/(K_d + X)$ for one site binding, where *B_{max}* is the maximal binding and the *K_d* is the concentration of ligand (in this case the LLY) necessary to achieve half-maximal binding. Data analysis was carried out using Graphpad Prism software.

Platelet Aggregation Assay. Platelet-rich plasma (PRP) was prepared from normal human donors as described previously (16). Blood donors were free of aspirin or other antiplatelet medications for at least 7 days prior to donation. Aggregation experiments were performed with a Model PAP-4 aggregometer from Bio/Data Corp. Total reaction volume was 200 μ L. Convulxin-induced aggregation (500 ng/mL final concentration (16)) was used as a positive control. LLY was assayed at 71 nM, LLY^{CDC} at 95 nM, and LLY^{Lec} at 280 nM.

Calcein Release Assay. PRP was diluted 1:100 with HEPES/saline assay buffer (2 mM CaCl₂, 1 mM MgCl₂, 150 mM NaCl, 10 mM HEPES, pH 7.5) and incubated with 2 μ M calcein acetoxymethyl ester (Molecular Probes, Eugene, OR) for 10 min at room temperature as previously described (17). LLY (0.7–2.9 nM) was incubated with the calcein-loaded PRP for 10 min at room temperature. Samples were then diluted with HEPES/saline and analyzed on a FACS-Calibur flow cytometer (Becton-Dickinson) using settings as described previously (17). Cells losing calcein fluorescence were quantified as a percentage of total platelets.

The EC₅₀ values for LLY- and LLY^{CDC}-dependent calcein release were calculated using a nonlinear sigmoidal dose-response curve fit of the data (Prism Software).

Glycan Microarray Binding Assay and Scanning. Glycan microarrays were prepared as described previously (33, 37) and obtained from the NIH/NIGMS-funded Consortium for Functional Glycomics (see <http://www.functionalglycomics.org/static/index.shtml>). Before assay, the slides were rehydrated for 5 min in TSM buffer (20 mM Tris-HCl, 150 mM sodium chloride (NaCl), 0.2 mM calcium chloride (CaCl₂), and 0.2 mM magnesium chloride (MgCl₂)). Alexa-

FIGURE 1: Primary structure of LLY. (a) The primary structure of LLY and its comparison with the primary structures of ILY and PLY. Comparison of the primary structure of LLY^{Lec} with that of the (b) *A. anguilla* agglutinin (AAA) (10) and (c) the glycan binding domain of the family 98 glycoside hydrolases from *S. pneumoniae* (SP2159) (19). The letters above the LLY sequence in panel a represent the amino acid differences with the GenBank sequence of Sm-hPAF (accession number AB051299.1). Homology comparisons were carried out using CLC Free Workbench version 4.6 (CLCBio). The conserved undecapeptide sequence of the CDCs is boxed in panel a. The conserved active site residues of AAA are bolded and underlined in panels b and c. Conserved residues (*), conservative substitutions (:).

Liposome Preparation. Cholesterol—phosphatidylcholine (55/45 mol %) liposomes were prepared as previously described (13). Lipids and cholesterol were obtained from Avanti Polar Lipids.

The Primary Structure of LLY. The LLY gene was cloned from *S. mitis* SK597, which exhibits characteristics of both *S. mitis* and *Streptococcus oralis* (Hollingshead, unpublished data). The gene sequence (see GenBank accession number EU597013) exhibits the typical AT-rich (60% A-T) sequence of streptococcal genes. The deduced primary structure of LLY is nearly identical to the GenBank sequence for SmhPAF from *S. mitis* Nm-65 (accession number AB051299.1); 12 mostly conservative amino acid differences were identified (Figure 1a). These differences did not result from PCR-generated errors in the LLY sequence reported herein; the same sequence was derived from the cloned products of two separate PCR amplification experiments. Hence, the primary structure of LLY can apparently vary to some extent. The open reading frame encodes a protein with a mass of 73780.3 Da. Based on the previously published amino-terminal sequence of purified protein from the supernatant of *S. mitis* NM-65 (7) the amino terminus of secreted LLY is located at or near Thr-37, which is preceded by a 36-residue peptide that exhibits a typical type II signal peptide structure. The primary structure of LLY from residue 199 to 665 (Figure

Table 1: Hemolytic Activity of LLY and Related CDCs Used in This Study^a

CDC	HD ₅₀ (pM)
ILY	1.1
PFO	0.8
LLY	4.1
LLY ^{CDC}	4.4

^a The relative HD₅₀ (hemolytic dose for 50% lysis of a standard erythrocyte suspension; see Methods) for each CDC used in these studies is provided.

1a) is most closely related to CDCs from *S. intermedius* (ILY) and *S. pneumoniae* (PLY). The CDC structure of LLY also contains an undecapeptide sequence (EKTGLVWEPWR) that is similar to the hallmark consensus sequence (ECTGLAWWWWR) found in most CDCs but contains substitutions at positions similar to those found in ILY (GATGLAWWWWR).

Unlike other characterized CDCs LLY contains an extra 162-residue peptide fused to its amino terminus (excluding the signal peptide) (Figure 1a). This peptide region exhibits similarity with the *A. anguilla* (European eel) agglutinin (AAA) (33% identity) (10) (Figure 1b) and the carboxy-terminal carbohydrate-binding module of a putative member of the family 98 glycoside hydrolases from *S. pneumoniae* (47% identity) (Figure 1c) (19). Both proteins are fucose-binding proteins that exhibit a preference for glycans containing the H-antigen structure (Fuc α 1–2Gal β 1–3(4)-GlcNAc-R).

Distribution of the LLY Gene. A collection of 165 strains of mostly *mitis* group streptococci was examined for the presence of the LLY gene by PCR using primers that encompassed its complete coding region. From this collection, twelve *S. mitis* strains, one *S. pneumoniae*, four *Streptococcus pseudopneumoniae*, and three *S. mitis/oralis* strains carried the gene. The PCR product size did not vary in size for any of the positive strains and comigrated with the 2 kb marker, consistent with its 1998 base pair sequence (including the stop codon) (data not shown). We confirmed expression and secretion of LLY in the SK597 strain (data not shown) that served as the source of the gene for our studies but have not confirmed its expression in the other species and strains that appear to carry the gene.

Hemolytic Activity of LLY and Derivatives. The coding region for LLY was cloned, expressed in *E. coli*, and purified (see Methods). Shown in Table 1 is the HD₅₀ (dose of toxin required for 50% hemolysis under standard conditions; see Methods) for purified LLY, LLY^{CDC} (LLY lacking the amino-terminal lectin domain), PFO, and ILY. In Table 1 are the HD₅₀ values, using human erythrocytes, for LLY and LLY^{CDC} and, for comparison, those of PFO and ILY. All of the CDCs exhibit picomolar HD₅₀ values, but it appears LLY and LLY^{CDC} are 4–5-fold less active than PFO and ILY. These values are within the typical range for these toxins and can vary depending on the cell type and species of origin. As described below, however, the amino-terminal lectin domain appears to exert a glycan-dependent enhancement of LLY activity with platelets.

Similar to other CDCs LLY and LLY^{CDC} also formed large oligomeric complexes on cholesterol-rich liposomes (Figure 2). LLY^{CDC} monomer (52147 Da) and oligomer migrated similarly to PFO monomer (52672 Da) and oligomer. The

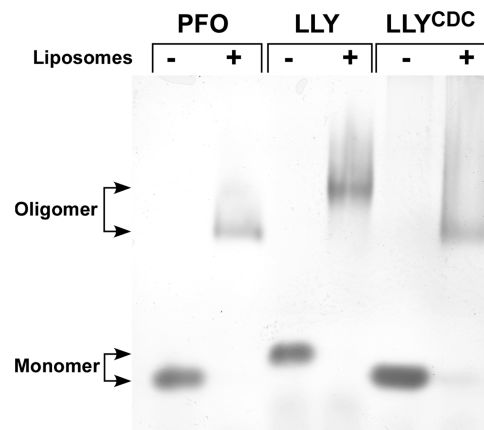


FIGURE 2: Oligomer formation by LLY. Purified PFO, LLY, and LLY^{CDC} were incubated in the absence and presence cholesterol-rich liposomes, and the monomer and oligomer species were separated by SDS–AGE. Shown is the Coomassie stained gel. The smearing of the oligomer bands results from the presence of the liposome-derived lipids in the oligomer samples.

similarity in the mass of both proteins suggests that both form oligomers with similar numbers of monomers. In contrast to PFO and LLY^{CDC} the migration of the LLY oligomer was significantly retarded. The slower migration of LLY was likely due to the additional mass contributed by the amino-terminal lectin domain (17751 Da). The CDCs typically form oligomers of 35–40 monomers (20); thus the oligomer mass of LLY would be at least 600 kDa greater than that of LLY^{CDC} or PFO, consistent with its slower migration on the gel.

LLY and Other CDCs Do Not Aggregate Platelets. Ohkuni et al. (7) reported that LLY (Sm-hPAF) stimulated platelet aggregation in human platelet-rich plasma (PRP). Qualitative analysis of platelet aggregation is commonly determined using an aggregometer, an instrument that measures the decrease in the light scattering properties of PRP as platelets aggregate into large complexes. Aggregometer analysis herein also showed apparent LLY-dependent platelet aggregation resulting in the decreased light scatter by the platelets (Figure 3a). Similar results were observed with purified LLY^{CDC}, demonstrating that the predicted amino-terminal fucose-binding lectin domain was not required for this activity (Figure 3a). Purified lectin domain (LLY^{Lec}) did not induce any change in the light scattering properties of the platelets (Figure 3a). To confirm the aggregometer measurements reflected platelet aggregation by LLY and LLY^{CDC}, we performed a microscopic examination of the platelets after treatment. Surprisingly, we could not identify any aggregated platelets (Figure 3b). By comparison, we observed large platelet aggregates in PRP treated with convulxin, a nonenzymatic glycoprotein from venom of *Crotalus durissus terrificus* that induces platelet aggregation. Although the aggregometer readings indicated that LLY and LLY^{CDC} could aggregate platelets, the microscopic examination did not support this interpretation. Although unlikely, it was possible that we simply missed the aggregates formed by LLY. Therefore, we quantified the relative levels of platelets in each preparation.

To measure the relative levels of platelets present in these mixtures, we utilized a flow cytometry based approach. PRP was either left untreated or treated in the aggregometer with 140 nM LLY or 500 ng/mL convulxin for 3 min at 37 °C

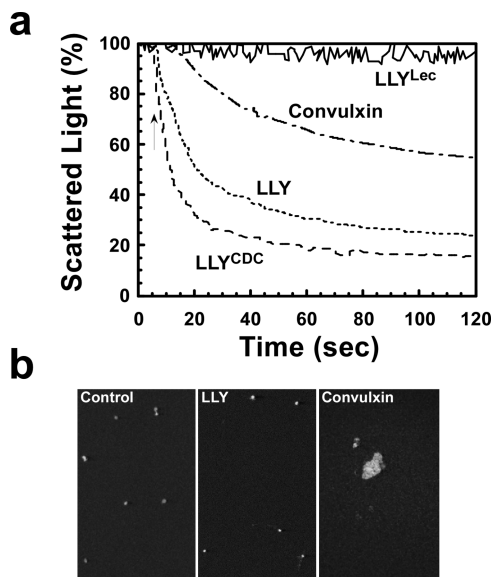


FIGURE 3: Platelet aggregation by LLY. Shown in (a) are the aggregometer recordings for platelets treated with LLY (71 nM), LLY^{CDC} (95 nM), and LLY^{Lec} (280 nM) and the positive control convulxin (500 ng/mL). Shown in (b) are confocal microscopic images of untreated, LLY-treated, and convulxin-treated platelets. These fields are representative of 12 separate fields.

with stirring. Aliquots of treated PRP were then incubated with FITC-labeled antiglycoprotein IIb/IIIa antibody, and platelet concentration was determined by flow cytometry. The relative platelet concentration in each sample was determined by the time required to accumulate 5000 events on the cytometer. If platelets aggregated into larger complexes, it would take longer to accumulate 5000 counts. If no significant aggregation occurs, then the time required for 5000 counts should be similar to untreated platelets. The LLY-treated and control (untreated) samples had nearly identical platelet concentrations (5000 counts/34 s and 5000 counts/31 s, respectively). In contrast, the convulxin-treated sample was significantly depleted of individual platelets (5000 counts/84 s). Hence, both convulxin and LLY induce changes in the light scattering properties of the platelets, but it is clear that LLY does not induce platelet aggregation. How then did LLY affect the light scattering properties of the platelets without aggregation?

The light scattering properties of cells often result from shape change and/or loss of cytoplasmic contents. For example, erythrocytes lose their light scattering properties upon pore formation by the CDC PFO (21). Pore formation in platelets was determined by monitoring calcein release from LLY-treated platelets. As shown in Figure 4, calcein is efficiently released in a dose-dependent manner from the platelets treated with LLY or with LLY^{CDC}, suggesting that each formed a membrane pore. The relative EC₅₀ for calcein release by both proteins was quantified below in the studies described in Figure 7, where we show that LLY exhibits variable activity on platelets from different donors.

To assess whether the observed change in light scattering properties of LLY in the aggregometer was dependent on pore formation, a mutant of LLY was trapped in the prepore complex by the introduction of an engineered disulfide, but which could be converted to the pore-forming oligomer by reduction of this bond. We previously showed a disulfide bridge between domains 2 and 3 of the CDC structure

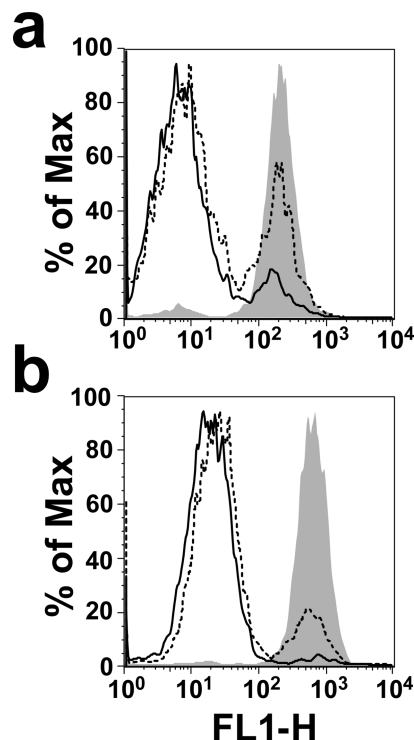


FIGURE 4: Calcein release from LLY-treated platelets. Calcein-loaded platelets were assayed by flow cytometry before (shaded peak) and after treatment with 0.7 nM (dashed line) or 1.4 nM (solid line) LLY (a) or LLY^{CDC} (b).

prevents membrane insertion of the transmembrane β -hairpins but not binding and assembly of the prepore oligomer (22). When the disulfide bridge was reduced, the transmembrane β -hairpins inserted into the membrane and formed the pore.

A prepore-locked mutant of LLY was generated by introducing cysteines for Gly-222 and Asn-351 (LLY^{G222C/N351C}), residues analogous to Gly-83 and Ser-217 of ILY and to Gly-57 and Ser-190 of PFO, which were shown previously to form a disulfide and trap both toxins in prepore complexes (ref 22 and Soltani and Tweten, unpublished data). LLY^{G222C/N351C} functioned as expected; when the disulfide bond was oxidized, it was not hemolytic, whereas reduction of the disulfide restored near native hemolytic activity (data not shown). Treatment of PRP with oxidized LLY^{G222C/N351C} did not elicit a change in the light scattering properties of the platelets (Figure 5a), but reduction of the disulfide bond restored this activity. Similarly, the oxidized disulfide-locked variants of ILY (Figure 5b) and PFO (Figure 5c) did not change the light scattering properties of the platelets, whereas the reduced forms of each triggered significant changes. These data show that the changes in light scattering properties of platelets are dependent on the pore-forming properties of LLY, PFO, and ILY and are not the result of platelet aggregation.

Glycan Specificity and Affinity of the LLY Lectin Domain. We next determined if the putative fucose-binding lectin domain of LLY was functional. A glycan microarray of vertebrate-type glycans (see Methods for a link to the complete list of glycans on this array) was probed with fluorescently tagged LLY. The probe consisted of the cysteine-substituted mutant LLY^{Q190C} labeled with the maleimide derivative of Alexa-488 via the cysteine sulfhydryl

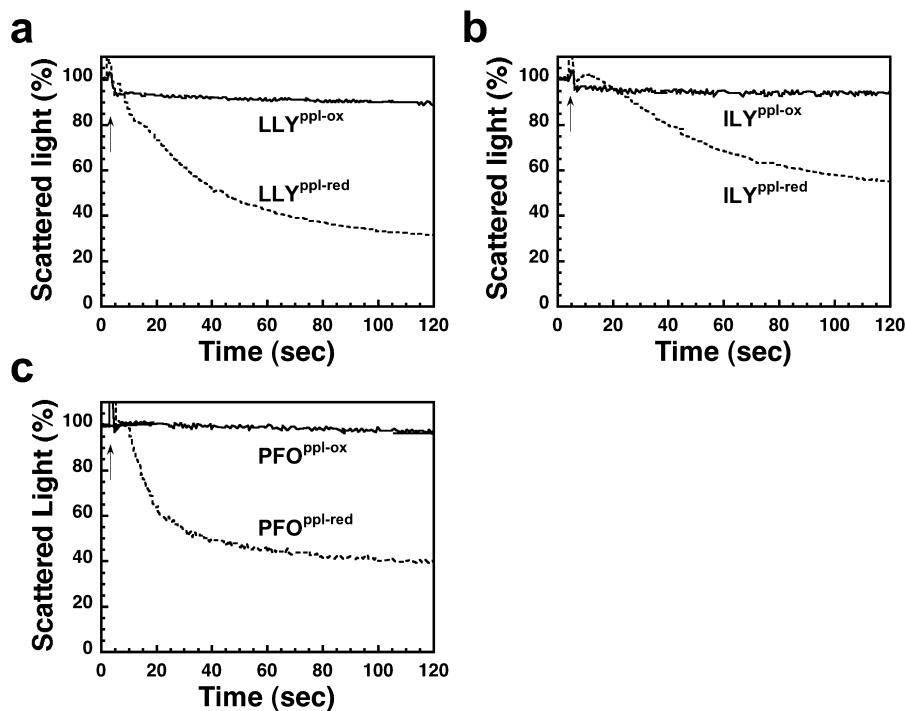


FIGURE 5: Platelet lysis requires pore formation. Shown are aggregometer readings for platelets treated with prepore locked mutants of LLY (a), ILY (b), and PFO (c) in their oxidized (LLY^{ppl-ox}, ILY^{ppl-ox}, and PFO^{ppl-ox}) and reduced forms (LLY^{ppl-red}, ILY^{ppl-red}, and PFO^{ppl-red}). Conditions were similar to those in Figure 3a; all toxins were added at approximately 70 nM. The reduction of the disulfide allows each prepore-locked mutant to convert to the pore complex.

(LLY^{Q190C-Alexa}). Gln-190 was chosen for substitution with cysteine since it is located at the junction of the CDC and lectin domains. When the glycan microarray was probed with LLY^{Q190C-Alexa}, no significant binding was detected (Figure 6a). This result suggested several possibilities: the lectin domain might bind to glycans that were not represented in the array, the lectin domain was not functional, or the glycan-binding site was sterically occluded or somehow inhibited in the soluble monomer of LLY.

We first tested the latter possibility, primarily because of the amino-terminal location of the lectin domain. This location positions the lectin domain distal to the carboxy-terminal domain 4, which contains the membrane-binding site of the CDCs (23–26). If the glycan-binding site was exposed in the monomer, it could bind LLY to cells in an unfavorable orientation, preventing critical domain 4 membrane interactions that initiate a cascade of ordered structural changes in the CDCs that lead to pore formation (reviewed in ref 27). Therefore, in this scenario occlusion or inhibition of the glycan-binding site may be necessary until after LLY has bound to the membrane. If correct, then expression of the lectin domain alone should restore its binding activity. A pair of stop codons was introduced after residue 190 of LLY^{Q190C} to eliminate the translation of the downstream CDC structure. This construct was designated LLY^{Lec-Q190C}.

Purified LLY^{Lec-Q190C} was fluorescently labeled with Alexa-488 and used to probe the glycan microarray. As shown in Figure 6b, we observed significant binding to several glycans on the microarray. We also determined whether binding to the glycans on the glycan microarray was lost if we changed a residue that has been shown to be conserved in the fucose-binding site of related lectins. The AAA glycan binding site contains three key residues that make polar contacts with the fucose molecule. The Nε of His-52 contacts O-5 of the

fucose ring whereas the guanidinium groups of Arg-79 and Arg-86 make contact with 3-OH and 4-OH ring hydroxyls of fucose (10). These residues are also conserved in the fucose-binding site of the family 98 glycoside hydrolases from *S. pneumoniae* (SP2159) (19) and correspond to residues His-85, Arg-112, and Arg-120 of LLY, respectively (Figure 1b,c). Arg-112 of LLY^{Lec} was changed to Ala in LLY^{Lec-Q190C}. This mutant (LLY^{Lec-Q190C/R112A}) was labeled with Alexa-488 at Cys190 and used to probe the glycan microarray. This mutation eliminated the glycan binding activity of LLY^{Lec} (Figure 6c), consistent with the conservation of this active site residue.

We further investigated the binding of LLY^{Lec} to the glycan microarray to determine its glycan specificity. We probe the microarray with three different concentrations of LLY^{Lec} that spanned a 100-fold range of concentration from 5.6 to 560 nM. These results (Table 2) are shown for all glycans bound at the highest concentration of LLY^{Lec} and selected glycans representative of those not bound by LLY^{Lec} at the highest concentration of LLY^{Lec} (representative of most glycans on the array). When the array was probed at 560 nM LLY^{Lec}, it bound to glycans containing the H-antigen structure (Fucα1–2Galβ1–3(4)GlcNAc-R) as found within the A, B, O, Le^y, and Le^b blood group antigens (Table 2, glycan IDs 1–24) and showed little affinity for the nonfucosylated type 1 and type 2 oligosaccharides (Table 2, glycan IDs 33–38), fucosylated glycans that did not contain the H-antigen, including Le^a and Le^x containing structures (Table 2, glycan IDs 27–32), and the difucosylated structures (Table 2, glycan IDs 42–50). At this high concentration of LLY^{Lec}, we observed some weak binding to irrelevant glycans (Table 1, glycan IDs 39–41). However, when the microarray was probed with 10-fold (56 nM) and 100-fold lower (5.6 nM) concentrations of LLY^{Lec}, we observed a marked shift in

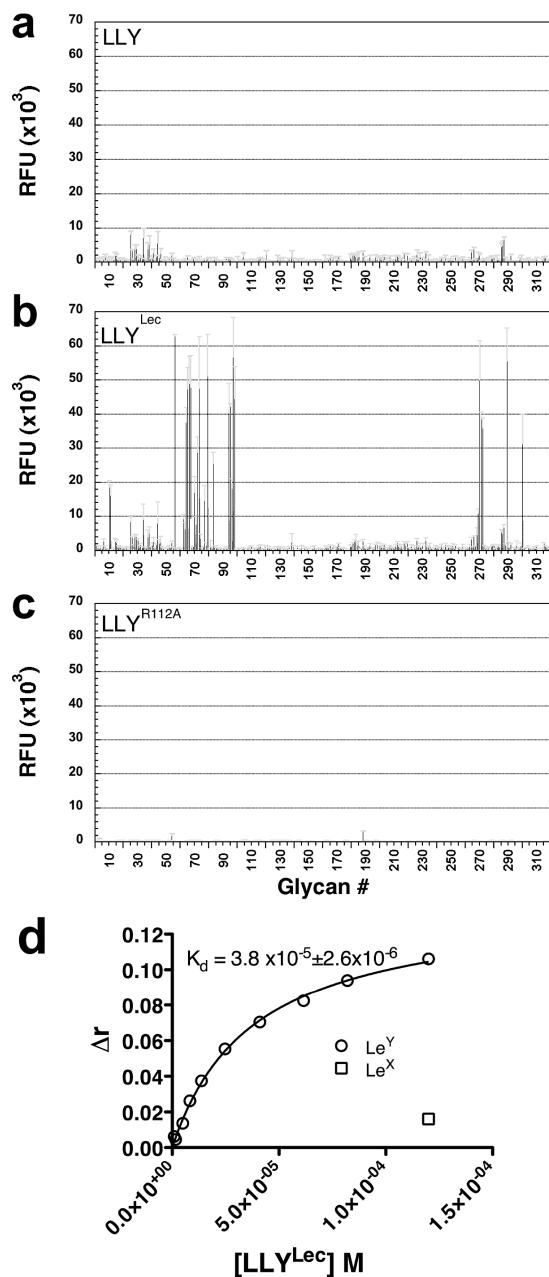


FIGURE 6: Glycan binding by LLY, LLY^{Lec}, and LLY^{Lec-R112A}. Version 3.0 of the printed glycan microarray, containing 320 eukaryotic-derived glycans (see Methods for a link to the full list of glycans on this array), was probed with fluorescently tagged (Alexa-488) versions of (a) LLY (670 nM), (b) LLY^{Lec} (560 nM), and (c) LLY^{Lec-R112A} (560 nM) that had been labeled at the cysteine-substituted Gln-190. Standard error of the mean is shown as gray error bars. Note: The microarray analyses herein were carried out using the updated version 3.0 of the glycan array whereas the results in Table 2 were obtained using version 2.1. This was a result of a change in the microarray version during the course of these studies. There are only five differences in fucose-containing glycans in the two versions. Only two of these glycans, numbers 290 and 301 on the version 3.0 array, contain the H-antigen structure and were shown to be bound by LLY^{Lec} whereas the other three glycans were not (data not shown). In panel d the K_d of the Le^y–LLY^{Lec} interaction was determined by measuring changes in the anisotropy (Δr) of Le^y (kept constant at 167 nm) in the presence of LLY^{Lec} that was varied from 300 nM to 120 μ M. Le^y incubated with the highest concentration of LLY (120 μ M) exhibited a Δr of $\approx 10\%$ of that observed for Le^y.

binding preference for glycans containing Le^y and Le^b antigens (Table 2, glycan IDs 1–7). These results demon-

strate that LLY^{Lec} has a unique recognition of difucosylated glycans Fuc α 1–2Gal β 1–3/4(Fuc α 1–4/3)GlcNAc-R) as found in Le^b and Le^y blood group antigens. Interestingly, glycans 6 and 7 are such difucosylated glycans, which also contain the blood group B and A determinants, respectively. However, as noted above, when the array is probed at the lowest concentration of LLY^{Lec}, it binds weakly or not at all to blood group B (Gal α 1–3[Fuc α 1–2]Gal β 1–3/4R), blood group A (GlcNAc α 1–3[Fuc α 1–2]Gal β 1–3/4R), or blood group H (Fuc α 1–2Gal β) determinants that lack the necessary difucosylated structures.

The affinity of LLY^{Lec} for Le^y was determined by measuring changes in fluorescence anisotropy (Δr) of fluorescently tagged Le^y as the concentration of LLY^{Lec} was varied. From this analysis the K_d of the LLY^{Lec}–Le^y interaction was determined to be approximately 38 μ M (Figure 6d). As expected from the microarray data, Le^x antigen, which lacks the H-antigen structure, was not bound significantly ($<10\%$ of Le^y) at the highest concentration of LLY^{Lec}.

The Lectin Domain of LLY Modulates Its Pore-Forming Activity. Ohkuni et al. (7) previously showed that platelets of some donors were unresponsive to Sm-hPAF-mediated aggregation (shown herein to be due to pore-dependent changes in platelet light scattering properties). This observation suggested that different donor platelets might exhibit different susceptibilities to the pore-forming activity of LLY. Consistent with this prediction, we observed that platelets from different donors exhibited differential susceptibility to LLY (Dale and Friese, unpublished observations). Shown in Figure 7a is the EC₅₀ for LLY pore formation determined on high (donor 1) and low (donor 3) sensitivity platelets. The platelets from donor 1 are nearly 6-fold more sensitive to LLY (EC₅₀ = 4.890×10^{-11}) than those from donor 3 (EC₅₀ = 2.88×10^{-10}). These results suggested that a feature of donor 1 platelets significantly enhanced their susceptibility to LLY.

We hypothesized that enhancement of LLY activity resulted from a glycan-dependent interaction of the lectin domain after monomer bound the cell surface. If correct, then preincubating platelets with LLY^{Lec} should prevent interaction of the lectin domain of LLY with surface glycans and block the enhancement of LLY activity on the highly sensitive donor 1 platelets. The EC₅₀ for calcein release by LLY from platelets pretreated with LLY^{Lec} (EC₅₀ = 3.8×10^{-10}) was approximately 8-fold higher than the EC₅₀ for LLY on platelets that were not pretreated with LLY^{Lec} (EC₅₀ = 4.890×10^{-11}) (Figure 7a). Similar results were observed if the platelets were incubated with 50 mM fucose instead of LLY^{Lec} but not with 50 mM sucrose as a control (data not shown). Furthermore, pretreatment of the low sensitivity donor 3 platelets with LLY^{Lec} had little impact on the activity of LLY, suggesting that the glycan(s) was largely absent from this donor's platelets. The results show the lectin domain increases LLY specific activity, apparently by interacting with one or more glycans on the cell surface of platelets.

These data also predict LLY^{CDC}, which lacks the lectin domain, should be less active than LLY on donor 1's platelets. To test this prediction, the EC₅₀ for calcein release by LLY and LLY^{CDC} was determined. As is shown in Figure 7b the EC₅₀ for LLY^{CDC} on donor 1 platelets was 7-fold higher than the EC₅₀ for LLY, consistent with the change

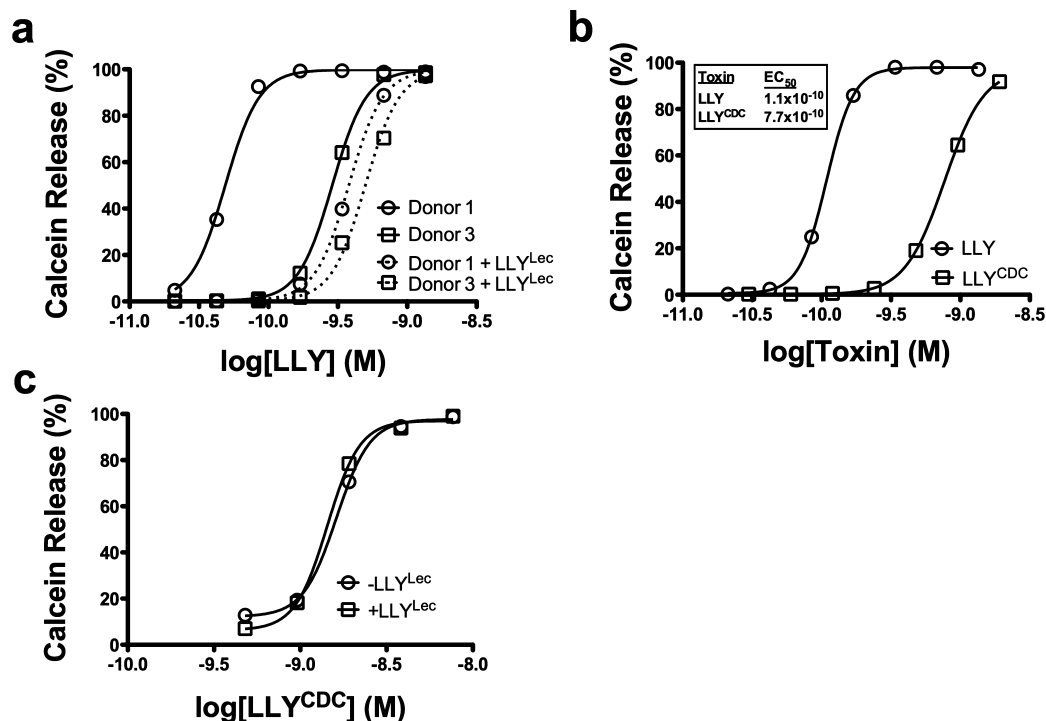


FIGURE 7: The glycan-binding domain of LLY modulates pore-forming activity. LLY-dependent calcein release from calcein-loaded PRP was measured by flow cytometry. (a) LLY-dependent calcein release from platelets of high (donor 1) and low responding donors (donor 3) which were preincubated without (solid lines) or with (dashed lines) LLY^{Lec} (56 nM). No change is observed with LLY^{Lec} alone (not shown). (b) Calcein release from platelets treated with LLY or LLY^{CDC}. (c) Same as the experiments shown in (a) with donor 1 platelets except that LLY^{CDC} was substituted for LLY.

observed in LLY activity on LLY^{Lec}-pretreated donor 1 platelets. Furthermore, LLY^{CDC} platelet pore-forming activity was not affected by preincubating the platelets with LLY^{Lec} (Figure 7c).

DISCUSSION

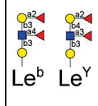
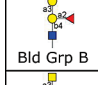
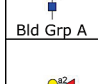
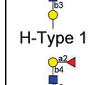
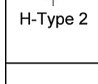

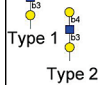
The studies herein show LLY is a functional CDC with an amino-terminal fucose-binding lectin domain. The LLY gene was detected in various isolates of the *mitis* group of the streptococci. This was not surprising, since there is evidence for the extensive exchange of genetic material between these species (28) and recently it has been shown that some *S. mitis* strains carry a gene encoding a CDC nearly identical to pneumolysin (6). Hence, it is perhaps not unexpected that the LLY gene appears to be present in one isolate of *S. pneumoniae*. LLY exhibits the typical large oligomeric membrane complexes and pore-forming activity of the CDCs. Pore formation in the platelet membrane was shown herein to be responsible for changes in their light scattering properties rather than the previously reported aggregation (7). The primary structure of LLY is distinct from other CDCs due to the presence of an amino-terminal fucose-binding lectin domain. The isolated lectin domain binds to glycans that contain H-antigen structure (Fuc α 1–2Gal β 1–3(4)GlcNAc-R), with a marked preference for the difucosylated Le^y and Le^b antigens. The glycan binding site is occluded in the soluble LLY monomer but is apparently exposed after the monomer binds to the cell surface since it enhances LLY-dependent pore-forming activity through a glycan-dependent mechanism. To date, LLY is the only characterized CDC to exhibit a glycan-binding lectin domain.

The glycan-binding site is occluded in the soluble LLY monomer, presumably to prevent nonproductive interactions

that would inhibit the assembly of the oligomeric pore complex. Previous studies showed that the CDC monomer is bound in a perpendicular orientation to the membrane surface via loops at the tip of domain 4, an interaction that initiates ordered conformational changes in the CDC structure necessary for pore formation (reviewed in ref 27). The amino-terminal location of the lectin domain places it next to domain 1 of the CDC structure and distal to the membrane-binding site in domain 4 (Figure 8). If the glycan-binding site was exposed in the soluble monomer, its interaction with a surface glycan could bind LLY to the surface in a nonproductive orientation that would prevent the assembly of the oligomeric pore complex. Yet, as described below, the glycan-binding site must be exposed after LLY binds to the membrane surface, since it enhances pore-forming activity.

Although caution must be used in extrapolating conclusions from molecular models, they suggest a possible explanation for the occlusion of the glycan-binding site in LLY. The structural model of the LLY^{Lec}, based on the crystal structure of the Le^y-binding module of *S. pneumoniae* family 98 glycoside hydrolase (19), positions the C-terminus of LLY^{Lec} on the same face as Arg-112, a residue we showed herein is conserved and essential for glycan binding. In LLY the carboxy-terminal lectin domain would be fused to the amino terminus of the CDC, orienting the binding site toward the upper surface of domain 1 of the CDC structure, potentially occluding the glycan-binding site. An assessment of the packing quality of the LLY^{CDC} structural model using ANOLEA (29) shows that residues in domain 1 (Figure 8), near the predicted site of interaction between the amino-terminal fucoselectin domain and domain 1 of the CDC, exhibit a nonfavorable energy environment. This suggests that these

Table 2: LLY^{Lec} Preferentially Binds Le^y and Le^b Glycans^a

Glycan Family	Glycan #	Glycan Structure	560 nM		56 nM		5.6 nM	
			AVG RFU	%CV	AVG RFU	%CV	AVG RFU	%CV
 Le ^b Le ^y	1	Fuca1-2Galβ1-4(Fuca1-3)GlcNAcβ-Sp8	42035	1004	50113	18	16748	3
	2	Fuca1-2Galβ1-4(Fuca1-3)GlcNAcβ-Sp0	52303	8	40704	6	15357	11
	3	Fuca1-2Galβ1-3(Fuca1-4)GlcNAcβ-Sp8	44801	7	44960	9	11763	5
	4	Fuca1-2Galβ1-4(Fuca1-3)GlcNAcβ1-3Galβ1-4(Fuca1-3)GlcNAcβ-Sp0	42253	4	54171	10	9445	10
	5	Fuca1-2Galβ1-4(Fuca1-3)GlcNAcβ1-3Galβ1-4(Fuca1-3)GlcNAcβ-Sp0	49653	11	54594	11	9201	3
	6	Gala1-3(Fuca1-2)Galβ1-4(Fuca1-3)GlcNAcβ-Sp0	43236	3	39872	2	9022	5
	7	GalaNAcα1-3(Fuca1-2)Galβ1-4(Fuca1-3)GlcNAcβ-Sp0	45556	4	37850	1	5506	2
 Bld Grp B	8	Gala1-3(Fuca1-2)Galβ-Sp8	42263	30	28788	6	2936	5
	9	Gala1-3(Fuca1-2)Galβ1-4Glcβ-Sp0	55729	9	11208	14	846	26
	10	Gala1-3(Fuca1-2)Galβ1-3GlcNAcβ-Sp0	35310	5	9312	19	743	17
	11	Gala1-3(Fuca1-2)Galβ1-4GlcNAcβ-Sp0	9081	8	2701	9	338	26
 Bld Grp A	12	GalaNAcα1-3(Fuca1-2)Galβ-Sp8	13806	9	3635	14	282	18
	13	GalaNAcα1-3(Fuca1-2)Galβ1-3GlcNAcβ-Sp0	203	18	247	34	304	59
	14	GalaNAcα1-3(Fuca1-2)Galβ1-4Glcβ-Sp0	617	11	302	36	97	12
 H-Type 1	15	Fuca1-2Galβ-Sp8	51057	11	17066	19	1443	13
	16	Fuca1-2[6OSO3]Galβ1-4[6OSO3]Glc-Sp0	35842	10	12584	14	486	47
	17	Fuca1-2-Galβ1-4[6OSO3]Glc-Sp0	23604	8	9152	9	176	65
	18	Fuca1-2Galβ1-4Glcβ-Sp0	17933	1	5716	12	537	14
	19	Fuca1-2Galβ1-4GlcNAcβ-Sp0	13896	12	3452	17	327	13
	20	Fuca1-2-(6OSO3)-Galβ1-4Glc-Sp0	13295	15	2345	90	56	42
	21	Fuca1-2Galβ1-3GlcNAcβ-Sp0	8226	10	1727	19	214	8
	22	Fuca1-2Galβ1-4GlcNAcβ-Sp8	7311	8	2133	14	164	73
	23	Fuca1-2Galβ1-3GlcNAcβ-Sp8	5908	16	1845	25	276	22
	24	Fuca1-2Galβ1-4[6OSO3]GlcNAcβ-Sp8	5045	10	1175	13	147	36
 H-Type 2	25	Fuca1-2Galβ1-4GlcNAcβ1-3Galβ1-4GlcNAcβ-Sp0	135	27	478	40	208	40
	26	Fuca1-2Galβ1-3GlcNAcβ1-3Galβ1-4Glcβ-Sp8	215	42	163	33	135	33
	27	Fuca1-4GlcNAcβ-Sp8	189	134	211	80	78	37
	28	Galβ1-3(Fuca1-4)GlcNAcβ-Sp8	237	61	101	15	144	88
	29	Neu5Acα2-3Galβ1-3(Fuca1-4)GlcNAcβ-Sp8	116	41	212	26	112	37
	30	Fuca1-3GlcNAcβ-Sp8	169	52	164	38	232	26
	31	Galβ1-4(Fuca1-3)GlcNAcβ-Sp8	91	79	184	8	194	26
	32	Neu5Acα2-3Galβ1-4(Fuca1-3)GlcNAcβ1-3Galβ-Sp8	187	75	98	61	89	36
	33	Neu5Acα2-3Galβ1-4GlcNAcβ1-3Galβ1-4GlcNAcβ1-3Galβ1-4GlcNAcβ-Sp0	281	49	169	27	111	39
	34	Galβ1-4GlcNAcβ1-3Galβ1-4GlcNAcβ1-3Galβ1-4GlcNAcβ-Sp0	217	37	189	50	152	60
 Le ^a Le ^x	35	Galβ1-4GlcNAcβ1-3Galβ1-4GlcNAcβ-Sp0	183	26	120	35	170	48
	36	NeuAcα2-3Galβ1-3GlcNAcβ1-3Galβ1-4GlcNAcβ-Sp0	194	33	147	49	117	49
	37	Galβ1-3GlcNAcβ1-3Galβ1-4Glcβ-Sp10	340	77	170	60	172	34
	38	Galβ1-3GlcNAcβ1-3Galβ1-4GlcNAcβ-Sp0	333	123	123	37	79	79
	39	α-L-Fuc-Sp8	3038	14	1435	36	326	28
Other	40	[3OSO3]Galβ1-4[6OSO3]Glcβ-Sp8	2745	28	848	11	397	17
	41	Transferrin	4066	31	1679	34	905	20
	42	Galβ1-4(Fuca1-3)GlcNAcβ1-4Galβ1-4(Fuca1-3)GlcNAcβ1-4Galβ1-4(Fuca1-3)GlcNAcβ-Sp0	522	68	138	16	216	48
 Diffucosylated, lacking Blood Group H	43	NeuAcα2-3Galβ1-3(Fuca1-4)GlcNAcβ1-3Galβ1-4(Fuca1-3)GlcNAcβ-Sp0	407	28	171	25	122	51
	44	Galβ1-4(Fuca1-3)GlcNAcβ1-3Galβ1-3(Fuca1-4)GlcNAcβ-Sp0	649	97	490	46	169	42
	45	Galβ1-3(Fuca1-4)GlcNAcβ1-3Galβ1-3(Fuca1-4)GlcNAcβ-Sp0	254	111	215	46	155	67
	46	Galβ1-3(Fuca1-4)GlcNAcβ1-3Galβ1-4(Fuca1-3)GlcNAcβ-Sp0	223	40	167	49	197	27
	47	Galβ1-4(Fuca1-3)GlcNAcβ1-4Galβ1-4(Fuca1-3)GlcNAcβ-Sp0	234	31	418	24	229	37
	48	Neu5Acα2-6Galβ1-4GlcNAcβ1-3Galβ1-4(Fuca1-3)GlcNAcβ1-3Galβ1-4(Fuca1-3)GlcNAcβ-Sp0	422	104	158	18	93	32
	49	Galβ1-4GlcNAcβ1-3Galβ1-4(Fuca1-3)GlcNAcβ1-3Galβ1-4(Fuca1-3)GlcNAcβ-Sp0	105	34	166	31	137	29
	50	Neu5Acα2-3Galβ1-4(Fuca1-3)GlcNAcβ1-3Galβ1-4(Fuca1-3)GlcNAcβ1-3Galβ1-4(Fuca1-3)GlcNAcβ-Sp0	23	517	287	58	170	15

^a Version 2.1 of the printed glycan microarray (Consortium for Functional Glycomics) was probed with Alexa-488 labeled LLY^{Lec}-Q190C at 560, 56, and 5.6 nM. To demonstrate specificity of binding by LLY^{Lec}, all glycans that were bound at the highest LLY^{Lec} concentration are shown as well as related glycans that were not bound or weakly bound. The average RFU (from four or six analysis with high and low values eliminated) for each bound glycan was determined as described in Methods and the % CV (100 × standard deviation ÷ average) provides an indication of the precision of each measurement. All other glycans on the version 2.1 array probed at the highest concentration of LLY^{Lec} did not exhibit signals above background. AVG RFU is average relative fluorescence units; SP, spacer arm or linker between glycan and surface of the array; SP0, -CH₂CH₂NH₂; and SP8, -CH₂CH₂CH₂NH₂. Key: yellow circles, galactose; yellow squares, GalNAc; red triangles, fucose; blue squares, GlcNAc.

residues do not pack similarly to the analogous residues in ILY. Hence, the residues in this region may adopt a different conformation in LLY so that they can specifically interact with the glycan-binding surface of the lectin domain in the soluble monomer.

Our studies revealed that platelets from different donors responded differently to LLY-dependent pore formation. Ohkuni et al. also observed a similar phenomenon in their aggregation experiments (7) (which we now know to be due to platelet lysis). The EC₅₀ for LLY on the platelets of a high responder donor was about six times lower than that observed when the platelets from a low responder when they were treated with LLY. This difference was abolished if both sets of platelets were treated with the lectin-deficient LLY^{CD} or if high responder platelets were first treated with LLY^{Lec} or L-fucose before adding ILY. When the high responder platelets were pretreated with LLY^{Lec} to block its binding sites before the addition of LLY, we observed an approximately 8-fold increase in the EC₅₀. Hence, LLY exhibits an intrinsic pore-forming activity that is enhanced by the

presence of the lectin domain, apparently in a glycan-dependent manner. The most likely explanation for the differences in platelet sensitivity is that the levels of glycan recognized by the lectin domain differ in platelets from various donors. Based on the array analysis Le^y and/or Le^b antigens are likely candidates for these differences, but we cannot rule out the possibility that other fucose-containing glycans mediate this interaction. The mechanistic stage of the LLY pore-forming mechanism that is modulated by the lectin domain is not yet known but apparently occurs after the initial domain 4-mediated cell binding. Most toxins that have a lectin-like domain use it to bind to glycan-containing receptors (30–36), whereas the LLY lectin domain does not appear to participate in receptor recognition.

The glycan microarray analysis showed Le^y and Le^b are preferred ligands of the LLY lectin, with the H-antigen itself being a weaker ligand. The H-antigen is expressed in many cells and tissues of all individuals, but expression of Le^y and Le^b antigens is more restricted in adults. Besides being on erythrocytes and in body secretions (e.g., saliva), they are

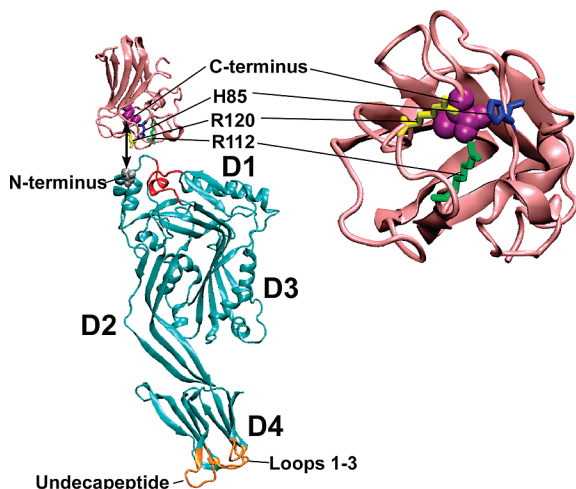


FIGURE 8: Molecular models of LLY^{CDC} and LLY^{Lec}. Shown are the ribbon representations of the LLY^{CDC} (cyan) and LLY^{Lec} (pink) molecular models generated by Swiss Model (swissmodel.expasy.org). The LLY^{CDC} model was generated using the ILY crystal structure (47) as the template whereas the LLY^{Lec} was modeled based on the structure of the Le^y-binding module of a *S. pneumoniae* virulence factor of the family 98 glycoside hydrolases (19). The locations are shown for the fucose-binding residues [His-85 (blue), Arg-112 (yellow), and Arg-120 (green)] and the C-terminal residue (space filled, magenta) of LLY^{Lec} and the amino-terminal residue of LLY^{CDC} (space filled, gray). The L1–L3 loops and undecapeptide at the tip of domain 4 are shown in gold. The red-colored regions of the LLY^{CDC} structural model exhibited a nonfavorable energy environment when analyzed with ANOLEA (29). Molecular structures were drawn with VMD (48).

expressed throughout the gastrointestinal tract but at levels that can differ based on location (37, 38). Expression of both antigens may be highly upregulated on epithelial tumors of the GI tract (39, 40). In normal tissue, Le^b is highly expressed on mucosal surfaces of the fetal colon, but in adults its expression is restricted to the proximal colon (41). Le^y is expressed strongly in proximal regions of the terminal ileum and cecum and weakly in the ascending colon and beyond (42). In addition, both Le^y and Le^b can be found weakly expressed in gastric mucosa (43). Le^y is also expressed by some *Helicobacter pylori* isolates (44).

Interestingly, Le^y is expressed at low levels in circulating human peripheral blood granulocytes but is upregulated upon their activation (45). Le^y-expressing neutrophils are also found in the synovial fluid of patients with arthritic joint disease (46). The *mitis* group of streptococci is part of the normal flora of the oropharynx and nasopharynx, but as indicated in the introduction they are increasingly associated with antibiotic-resistant bacteremia or septicemia. The lectin-dependent enhancement of LLY activity may increase its activity toward Le^y-expressing activated neutrophils, thus potentially blunting one of the early responses to infection.

In summary, these studies show that LLY is a member of the CDC family of pore-forming toxins and is the only identified CDC that has a glycan-binding lectin domain. The lectin domain exhibits a strong preference for Le^b and Le^y and modulates LLY pore-forming activity in a glycan-dependent manner after LLY has bound to the membrane. The mechanistic basis for this effect remains unknown. Finally, several species of streptococci appear to carry the gene for LLY. One *S. pneumoniae* isolate appeared to carry the gene for LLY, suggesting that there may be a subpopu-

lation of this important pathogen that expresses LLY in association with PLY or it has been substituted for PLY.

ACKNOWLEDGMENT

The excellent technical assistance of P. Coan is appreciated. The authors also acknowledge The Consortium for Functional Glycomics for support of the glycan array analysis and for providing the amino-derivatized Le^y and Le^x glycans for fluorescent derivatization.

REFERENCES

- Kennedy, M. J., Jackson, M. A., and Kearns, G. L. (2004) Delayed diagnosis of penicillin-resistant *Streptococcus mitis* endocarditis following single-dose amoxicillin prophylaxis in a child. *Clin. Pediatr. (Philadelphia)* 43, 773–776.
- Gowda, R. M., Ansari, A. W., and Khan, I. A. (2003) Complete endocardial cushion defect (complete atrioventricular canal) manifested in adult life by *Streptococcus mitis* endocarditis of the common atrioventricular valve. *Int. J. Cardiol.* 89, 109–110.
- Hall, G. E., and Baddour, L. M. (2002) Apparent failure of endocarditis prophylaxis caused by penicillin-resistant *Streptococcus mitis*. *Am. J. Med. Sci.* 324, 51–53.
- Huang, I. F., Chiou, C. C., Liu, Y. C., and Hsieh, K. S. (2002) Endocarditis caused by penicillin-resistant *Streptococcus mitis* in a 12-year-old boy. *J. Microbiol., Immunol., Infect. (China)* 35, 129–132.
- Lu, H. Z., Weng, X. H., Zhu, B., Li, H., Yin, Y. K., Zhang, Y. X., Haas, D. W., and Tang, Y. W. (2003) Major outbreak of toxic shock-like syndrome caused by *Streptococcus mitis*. *J. Clin. Microbiol.* 41, 3051–3055.
- Jefferies, J., Nieminen, L., Kirkham, L. A., Johnston, C., Smith, A., and Mitchell, T. J. (2007) Identification of a secreted cholesterol-dependent cytolysin (mitilysin) from *Streptococcus mitis*. *J. Bacteriol.* 189, 627–632.
- Ohkuni, H., Todome, Y., Okibayashi, F., Watanabe, Y., Ohtani, N., Ishikawa, T., Asano, G., and Kotani, S. (1997) Purification and partial characterization of a novel human platelet aggregation factor in the extracellular products of *Streptococcus mitis*, strain Nm-65. *FEMS Immunol. Med. Microbiol.* 17, 121–129.
- Ohkuni, H., Todome, Y., Takahashi, H., Nagamune, H., Abe, J., Ohtsuka, H., and Hatakeyama, H. (2006) Antibody titers to *Streptococcus mitis*-derived human platelet aggregation factor (SmhPAF) in the sera of patients with Kawasaki disease, in *Proceedings of the XVIth Lancefield International Symposium on Streptococci and Streptococcal Diseases* (Sriprakash, K. S., Ed.) pp 71–74, Elsevier B.V., Palm Cove, Australia.
- Nagamune, H., Whiley, R. A., Goto, T., Inai, Y., Maeda, T., Hardie, J. M., and Kourai, H. (2000) Distribution of the intermedilysin gene among the anginosus group streptococci and correlation between intermedilysin production and deep-seated infection with *Streptococcus intermedilysin*. *J. Clin. Microbiol.* 38, 220–226.
- Bianchet, M. A., Odom, E. W., Vasta, G. R., and Amzel, L. M. (2002) A novel fucose recognition fold involved in innate immunity. *Nat. Struct. Biol.* 9, 628–634.
- Majumder, S., Roy, A., and Mandal, C. (2004) Prediction of 3-D structures of fucose-binding proteins and structural analysis of their interaction with ligands. *Glycoconjugate J.* 20, 545–550.
- Giddings, K. S., Johnson, A. E., and Tweten, R. K. (2003) Redefining cholesterol's role in the mechanism of the cholesterol-dependent cytolysins. *Proc. Natl. Acad. Sci. U.S.A.* 100, 11315–11320.
- Shepard, L. A., Heuck, A. P., Hamman, B. D., Rossjohn, J., Parker, M. W., Ryan, K. R., Johnson, A. E., and Tweten, R. K. (1998) Identification of a membrane-spanning domain of the thiol-activated pore-forming toxin *Clostridium perfringens* perfringolysin O: an α -helical to β -sheet transition identified by fluorescence spectroscopy. *Biochemistry* 37, 14563–14574.
- Soltani, C. E., Hotze, E. M., Johnson, A. E., and Tweten, R. K. (2007) Specific protein-membrane contacts are required for prepore and pore assembly by a cholesterol-dependent cytolysin. *J. Biol. Chem.* 282, 15709–15716.
- Song, X., Xia, B., Lasanajak, Y., Smith, D. F., and Cummings, R. D. (2008) Quantifiable fluorescent glycan microarrays. *Glycoconjugate J.* 25, 15–25.

16. Alberio, L., Safa, O., Clemetson, K. J., Esmon, C. T., and Dale, G. L. (2000) Surface expression and functional characterization of alpha-granule factor V in human platelets: effects of ionophore A23187, thrombin, collagen, and convulxin. *Blood* 95, 1694–1702.
17. Remenyi, G., Szasz, R., Friese, P., and Dale, G. L. (2005) Role of mitochondrial permeability transition pore in coated-platelet formation. *Arterioscl., Thromb. Vasc. Biol.* 25, 467–471.
18. Shepard, L. A., Shatursky, O., Johnson, A. E., and Tweten, R. K. (2000) The mechanism of assembly and insertion of the membrane complex of the cholesterol-dependent cytolysin perfringolysin O: Formation of a large prepore complex. *Biochemistry* 39, 10284–10293.
19. Boraston, A. B., Wang, D., and Burke, R. D. (2006) Blood group antigen recognition by a *Streptococcus pneumoniae* virulence factor. *J. Biol. Chem.* 281, 35263–35271.
20. Czajkowsky, D. M., Hotze, E. M., Shao, Z., and Tweten, R. K. (2004) Vertical collapse of a cytolysin prepore moves its transmembrane β -hairpins to the membrane. *EMBO J.* 23, 3206–3215.
21. Harris, R. W., Sims, P. J., and Tweten, R. K. (1991) Kinetic aspects of the aggregation of *Clostridium perfringens* theta toxin on erythrocyte membranes: A fluorescence energy transfer study. *J. Biol. Chem.* 266, 6936–6941.
22. Hotze, E. M., Wilson-Kubalek, E. M., Rossjohn, J., Parker, M. W., Johnson, A. E., and Tweten, R. K. (2001) Arresting pore formation of a cholesterol-dependent cytolysin by disulfide trapping synchronizes the insertion of the transmembrane beta-sheet from a prepore intermediate. *J. Biol. Chem.* 276, 8261–8268.
23. Giddings, K. S., Zhao, J., Sims, P. J., and Tweten, R. K. (2004) Human CD59 is a receptor for the cholesterol-dependent cytolysin intermediates. *Nat. Struct. Mol. Biol.* 12, 1173–1178.
24. Heuck, A. P., Tweten, R. K., and Johnson, A. E. (2003) Assembly and topography of the prepore complex in cholesterol-dependent cytolysins. *J. Biol. Chem.* 278, 31218–31225.
25. Ramachandran, R., Heuck, A. P., Tweten, R. K., and Johnson, A. E. (2002) Structural insights into the membrane-anchoring mechanism of a cholesterol-dependent cytolysin. *Nat. Struct. Biol.* 9, 823–827.
26. Ramachandran, R., Tweten, R. K., and Johnson, A. E. (2005) The domains of a cholesterol-dependent cytolysin undergo a major FRET-detected rearrangement during pore formation. *Proc. Natl. Acad. Sci. U.S.A.* 102, 7139–7144.
27. Tweten, R. K. (2005) The cholesterol-dependent cytolysins; a family of versatile pore-forming toxins. *Infect. Immun.* 73, 6199–6209.
28. Kawamura, Y., Hou, X. G., Sultana, F., Miura, H., and Ezaki, T. (1995) Determination of 16S rRNA sequences of *Streptococcus mitis* and *Streptococcus gordonii* and phylogenetic relationships among members of the genus *Streptococcus*. *Int. J. Syst. Bacteriol.* 45, 406–408.
29. Melo, F., and Feytmans, E. (1998) Assessing protein structures with a non-local atomic interaction energy. *J. Mol. Biol.* 277, 1141–1152.
30. Merritt, E. A., Sixma, T. K., Kalk, K. H., van Zanten, B. A., and Hol, W. G. (1994) Galactose-binding site in *Escherichia coli* heat-labile enterotoxin (LT) and cholera toxin (CT). *Mol. Microbiol.* 13, 745–753.
31. Stein, P. E., Boodhoo, A., Armstrong, G. D., Cockle, S. A., Klein, M. H., and Read, R. J. (1994) The crystal structure of pertussis toxin. *Structure* 2, 45–57.
32. Olson, R., and Gouaux, E. (2005) Crystal structure of the *Vibrio cholerae* cytolysin (VCC) pro-toxin and its assembly into a heptameric transmembrane pore. *J. Mol. Biol.* 350, 997–1016.
33. Clark, G. F., Krivan, H. C., Wilkins, T. D., and Smith, D. F. (1987) Toxin A from *Clostridium difficile* binds to rabbit erythrocyte glycolipids with terminal Gal alpha 1–3Gal beta 1–4GlcNAc sequences. *Arch. Biochem. Biophys.* 257, 217–229.
34. Nestic, D., Hsu, Y., and Stebbins, C. E. (2004) Assembly and function of a bacterial genotoxin. *Nature* 429, 429–433.
35. Tateno, H., and Goldstein, I. J. (2003) Molecular cloning, expression, and characterization of novel hemolytic lectins from the mushroom *Laetiporus sulphureus*, which show homology to bacterial toxins. *J. Biol. Chem.* 278, 40455–40463.
36. Rossjohn, J., Buckley, J. T., Hazes, B., Murzin, A. G., Read, R. J., and Parker, M. W. (1997) Aerolysin and pertussis toxin share a common receptor-binding domain. *EMBO J.* 16, 3426–3434.
37. Hakomori, S. I., and Siddiqui, B. (1974) Isolation and characterization of glycosphingolipid from animal cells and their membranes. *Methods Enzymol.* 32, 345–367.
38. Marcus, D. M. (1969) The ABO and Lewis blood-group system. Immunochimistry, genetics and relation to human disease. *N. Engl. J. Med.* 280, 994–1006.
39. Inoue, M., Nakayama, M., and Tanizawa, O. (1990) Altered expression of Lewis blood group and related antigens in fetal, normal adult and malignant tissues of the uterine endometrium. *Virchows Arch.* 416, 221–228.
40. Heller, D. S., and Thung, S. N. (1990) Expression of Lewis(x) and Lewis(y) blood group related antigens in fetal livers. *Pediat. Pathol.* 10, 681–687.
41. Jass, J. R., and Robertson, A. M. (1994) Colorectal mucin histochemistry in health and disease: a critical review. *Pathol. Int.* 44, 487–504.
42. Abe, K., Hakomori, S., and Ohshiba, S. (1986) Differential expression of difucosyl type 2 chain (LeY) defined by monoclonal antibody AH6 in different locations of colonic epithelia, various histological types of colonic polyps, and adenocarcinomas. *Cancer Res.* 46, 2639–2644.
43. Sakamoto, S., Watanabe, T., Tokumaru, T., Takagi, H., Nakazato, H., and Lloyd, K. O. (1989) Expression of Lewisia, Lewisb, Lewisx, Lewisy, sialyl-Lewisx, and sialyl-Lewisx blood group antigens in human gastric carcinoma and in normal gastric tissue. *Cancer Res.* 49, 745–752.
44. Appelmelk, B. J., Simoons-Smit, I., Negrini, R., Moran, A. P., Aspinall, G. O., Forte, J. G., DeVries, T., Quan, H., Verboom, T., Maaskant, J. J., Ghiara, P., Kuipers, E. J., Bloemena, E., Tadema, T. M., Townsend, R. R., Tyagarajan, K., Crothers, J. M., Jr., Monteiro, M. A., Savio, A., and DeGraaff, J. (1996) Potential role of molecular mimicry between *Helicobacter pylori* lipopolysaccharide and host Lewis blood group antigens in autoimmunity. *Infect. Immun.* 64, 2031–2040.
45. Dettke, M., Palfi, G., and Loibner, H. (2000) Activation-dependent expression of the blood group-related lewis Y antigen on peripheral blood granulocytes. *J. Leukocyte Biol.* 68, 511–514.
46. Dettke, M., Palfi, G., Pursch, E., Fischer, M. B., and Loibner, H. (2001) Increased expression of the blood group-related Lewis Y antigen on synovial fluid granulocytes of patients with arthritic joint diseases. *Rheumatology (Oxford, England)* 40, 1033–1037.
47. Polekhina, G., Giddings, K. S., Tweten, R. K., and Parker, M. W. (2005) Insights into the action of the superfamily of cholesterol-dependent cytolysins from studies of intermediates. *Proc. Natl. Acad. Sci. U.S.A.* 102, 600–605.
48. Humphrey, W., Dalke, A., and Schulten, K. (1996) VMD: visual molecular dynamics. *J. Mol. Graphics* 14, 33–38, 27–38.

BI8005835